



Published in final edited form as:

*Oncogene*. 2015 June ; 34(26): 3452–3462. doi:10.1038/onc.2014.277.

## WNT7A/ $\beta$ -catenin signaling induces FGF1 and influences sensitivity to niclosamide in ovarian cancer

Mandy L. King<sup>1</sup>, Mallory E. Lindberg<sup>1</sup>, Genna R. Stodden<sup>1</sup>, Hiroshi Okuda<sup>2</sup>, Steven D. Ebers<sup>1</sup>, Alyssa Johnson<sup>3</sup>, Anthony Montag<sup>4</sup>, Ernst Lengyel<sup>3</sup>, James A. MacLean II<sup>1</sup>, and Kanako Hayashi<sup>1</sup>

<sup>1</sup>Department of Physiology, Southern Illinois University School of Medicine, Carbondale, IL

<sup>2</sup>Laboratory for Malignancy Control Research, Kyoto University Graduate School of Medicine, Kyoto, Japan

<sup>3</sup>Department of Obstetrics and Gynecology, Section of Gynecologic Oncology, The University of Chicago Medical Center, Chicago, IL

<sup>4</sup>Department of Pathology, The University of Chicago Medical Center, Chicago, IL

### Abstract

We previously characterized the link between WNT7A and the progression of ovarian cancer. Other groups have identified FGF1 as a relevant risk factor in ovarian cancer. Here, we show a linkage between these two signaling pathways that may be exploited to improve treatment and prognosis of patients with ovarian cancer. High expression of WNT7A and FGF1 are correlated in ovarian carcinomas and poor overall patient survival. A chromatin immunoprecipitation assay demonstrated that WNT7A/ $\beta$ -catenin signaling directly regulates *FGF1* expression via TCF binding elements in the *FGF1-IC* promoter locus. *In vitro* gene manipulation studies revealed that FGF1 is sufficient to drive the tumor promoting effects of WNT7A. *In vivo* xenograft studies confirmed that the stable overexpression of WNT7A or FGF1 induced a significant increase in tumor incidence, while FGF1 knockdown in WNT7A overexpressing cells caused a significant reduction in tumor size. Niclosamide most efficiently abrogated WNT7A/ $\beta$ -catenin signaling in our model, inhibited  $\beta$ -catenin transcriptional activity and cell viability, and increased cell death. Furthermore, niclosamide decreased cell migration following an increase in E-cadherin subsequent to decreased levels of SLUG. The effects of niclosamide on cell functions were more potent in WNT7A overexpressing cells. Oral niclosamide inhibited tumor growth and progression in an intraperitoneal xenograft mouse model representative of human ovarian cancer. Collectively, these results indicate that FGF1 is a direct downstream target of WNT7A/ $\beta$ -catenin signaling and this pathway has potential as a therapeutic target in ovarian cancer. Moreover, niclosamide is a promising inhibitor of this pathway and may have clinical relevance.

Users may view, print, copy, and download text and data-mine the content in such documents, for the purposes of academic research, subject always to the full Conditions of use:[http://www.nature.com/authors/editorial\\_policies/license.html#terms](http://www.nature.com/authors/editorial_policies/license.html#terms)

Correspondence: Kanako Hayashi, Department of Physiology, Southern Illinois University School of Medicine, 1135 Lincoln Drive, Carbondale, Illinois 62901. Tel: 618-453-1562, Fax: 618-453-1517, khayashi@siu.edu.

No potential conflicts of interest were declared.

### CONFLICT OF INTEREST

The authors declare no conflict of interest.

## Keywords

FGF1; WNT7A; WNT/ $\beta$ -catenin pathway; ovarian cancer; therapeutic target

---

## INTRODUCTION

Ovarian cancer (OvCa) remains the most common cause of death from gynecological malignancies and is the fifth leading overall cause of death from cancer in women. In 2014, approximately 22,000 new OvCa cases and 14,500 deaths are estimated from OvCa in the United States.<sup>1</sup> The dearth of specific signs, symptoms, or efficient early detection markers for this disease contributes to its diagnosis at advanced stages, resulting in low overall survival. Indeed, more than 75% of OvCa cases are diagnosed when there is widely metastatic disease in the peritoneal cavity.<sup>2</sup> Therefore, it is important to identify therapeutic targets and efficient drugs that can improve current OvCa treatment by preventing its dissemination.

*WNT* genes encode secreted glycoproteins, acting through frizzled receptor (FZD), that control cell fate, mortality, proliferation, differentiation and tissue growth.<sup>3, 4</sup> Gene mutations and changes in the expression of extracellular inhibitors and intranuclear transcription cofactors within the WNT pathway promote tumor progression and metastasis.<sup>5, 6</sup> The canonical pathway of WNT signaling results in the nuclear accumulation of  $\beta$ -catenin and transcriptional activation of target genes. WNT/ $\beta$ -catenin signaling plays a role in ovarian tumorigenesis,<sup>7</sup> as well as chemoresistance in cancer stem cells of all OvCa subtypes.<sup>8</sup> Our recent findings also suggest that the expression of WNT7A during the malignant transformation of OvCa plays a critical role in tumor progression mediated by the WNT/ $\beta$ -catenin signaling pathway.<sup>9</sup>

FGF1 is one of 23 members of the highly conserved polypeptide fibroblast growth factor family. FGF1 has strong mitogenic effects on a variety of different cell types in various stages of development, morphogenesis and angiogenesis in neoplastic or non-neoplastic tissues.<sup>10, 11</sup> FGF1 has been identified as a potential prognostic marker for OvCa.<sup>12</sup> Genetic variation of *FGF1* has the most significant association with increased OvCa risk within the FGF family.<sup>13</sup> Furthermore, *FGF1* expression is also a significant determinant of survival and response to platinum-based chemotherapy.<sup>14</sup> Thus, modulation of FGF1 by distinct mechanisms in OvCa may be important in ovarian tumor progression.

Nicosamide is an efficacious and minimally toxic, FDA-approved drug for the treatment of helminth parasites, specifically tapeworms, in humans. Several groups have reported that nicosamide is active against cancer cells and targets WNT signaling.<sup>15-19</sup> Nicosamide inhibits solid tumor growth in a colon cancer model by promoting FZD endocytosis, leading to the downregulation of DVL,  $\beta$ -catenin stabilization and TCF/LEF activity.<sup>17, 20</sup> Nicosamide inhibits tumor growth by targeting S100A4, which is a transcriptional target of WNT signaling,<sup>18</sup> and by suppressing LRP6 in prostate and breast cancer cells.<sup>15</sup> Given its proven safety record and mechanisms that target WNT signaling raises the possibility of repurposing nicosamide for OvCa treatment.

In the present study, we show that *WNT7A* and *FGF1* expression are highly correlated in ovarian carcinomas, and *FGF1* is a direct transcriptional target of *WNT7A*/β-catenin signaling. Niclosamide was an effective inhibitor of *WNT7A*/β-catenin signaling, including *FGF1* expression, and should be further explored as treatment for OvCa.

## RESULTS

### Analysis of *FGF1* in OvCa

While analysis of *FGF1* gene expression or variation has indicated an association with OvCa risk,<sup>12-14</sup> the expression pattern of *FGF1* in ovarian cancer has not been characterized. Therefore, immunoreactive *FGF1* was examined using human OvCa tissues. *FGF1* was low in normal (Figure 1a) and benign (Figure 1b) ovary, as well as benign fallopian tube epithelium (Figure 1c). *FGF1* was highly detected in high grade invasive serous epithelial carcinomas (Figure 1d, black arrows), and surface epithelial cells of low grade serous carcinomas (Figure 1e, black arrows). Heterogeneous *FGF1* was seen in the tumor microenvironment, with lymphocytes positive in serous (Figure 1f), but not in endometrioid carcinomas (Figure 1g). *FGF1* was observed in fibroblasts of several histotypes (Figure 1d, h, open white arrows). *FGF1* was positive in clear cell carcinomas (Figure 1h, black arrows). *FGF1* was specifically detected in non-invasive cells lining the basal membrane (Figure 1i, black arrows) and in the surface epithelial cells of mucinous carcinomas (Figure 1j). Abundant *FGF1* was also detected in epithelial fallopian tube carcinomas (Figure 1k, black arrows). *FGF1* was significantly higher in serous, clear cell, mucinous and fallopian tube primary carcinomas compared to normal/benign ovarian and fallopian tube tissues. Specifically, serous and fallopian tube carcinomas showed higher levels of *FGF1* than endometrioid carcinomas (Figure 1q). *FGF1* was observed in metastases from serous (Figure 1l, q), clear cell (Figure 1n, q), mucinous (Figure 1o, q) and fallopian tube (Figure 1p, q) carcinomas, but not from endometrioid carcinomas (Figure 1m, q).

### Correlation between *WNT7A* and *FGF1* levels and overall survival

Since *FGF* family members have previously been identified as downstream targets of *WNT* signaling,<sup>21</sup> and a role for the specific ligand *WNT7A* was elucidated in tumor growth and progression,<sup>9</sup> we next examined whether *WNT7A* is associated with *FGF1* in OvCa. A total of 41 fresh-frozen ovarian samples including 5 normal/benign, 25 serous, 8 endometrioid, 3 clear cell and 0 mucinous were examined for *WNT7A* and *FGF1* mRNA levels (Figure 2a). The expression of *WNT7A* in serous carcinomas was correlated with high levels of *FGF1* expression. Elevated *WNT7A* was correlated with moderately increased *FGF1* levels in clear cell carcinomas. Significantly higher *WNT7A* was observed in serous (1506-fold) and clear cell (231-fold), but not in endometrioid carcinomas compared to normal/benign ovaries. *FGF1* transcripts were significantly higher (48-fold) in serous carcinomas compared to normal/benign ovaries and slightly increased in clear cell carcinomas (6.26-fold), but unchanged in endometrioid carcinomas.

Using previously generated cell lines,<sup>9</sup> a correlation between *FGF1* and *WNT7A* was observed in cells with knockdown or overexpression of *WNT7A*, and in orthotopic tumors that developed from these cells (Figure 2b). However, no other *FGF* family members, nor

FGF receptors, appeared to consistently follow *WNT7A* expression (Supplementary Figures 1 and 2). To further explore the correlation between *WNT7A* and *FGF1* expression in OvCa, we evaluated the prognostic and predictive impact of *WNT7A* and *FGF1* using Gene Expression Omnibus (GEO) and The Cancer Genome Atlas (TCGA) datasets. A total of 961 primary ovarian tumors with completed data sets were selected for survival analysis. High expression of both *WNT7A* and *FGF1* was significantly correlated with poor survival as determined by log-rank test ( $P=0.0304$ , Figure 2c). Furthermore, the 5-year (60 months) survival rate was 34.2% in women with high *WNT7A* and *FGF1* expressing tumors as compared to 49.4% in women with low *WNT7A* and *FGF1* expressing tumors. These findings were similar to previously reported survival rates of advanced OvCa patients 5 years after initial diagnosis.<sup>22, 23</sup>

### **FGF1 is a direct transcriptional target of WNT7A/ $\beta$ -catenin signaling**

The *FGF1* gene is composed of a single protein isoform and has four alternative tissue-specific promoters subject to alternative splicing (Figure 3a).<sup>24, 25</sup> Each promoter is coupled with its 5' untranslated exon, giving rise to four mRNAs with distinct UTRs, containing exons *1A*, *1B*, *1C* and *1D*, respectively. Therefore, we examined specific *FGF1* transcript(s) in OvCa using 4 different forward primers designed in each untranslated exon and one reverse primer designed in exon 1. SKOV3.ip1 cells, which express high endogenous *WNT7A* and *FGF1* (Supplementary Figure 3), show low or no expression of transcripts *1A*, *1B* or *1D*, and high expression of the *1C* transcript (12-fold higher than that of *1A* and *1B* (Figure 3b)). The *1C* transcript was reduced in *WNT7A* knockdown SKOV3.ip1 cells, suggesting that *1C* is specific to OvCa and possibly regulated by *WNT7A*. Similarly, *FGF1-1C* was the most abundant transcript in human malignant ovarian tissues (Figure 3c).

To determine whether *FGF1* is likely to be a direct rather than indirect  $\beta$ -catenin/TCF target gene, we searched the *FGF1* genomic locus and flanking DNA sequences for consensus TCF/LEF-binding elements (WWCAAWG, W=A/T). We found several putative binding sites at the *1A*, *1B* and *1C* locus, but not at the *1D* locus (Figure 3a). Therefore, we performed chromatin immunoprecipitation (ChIP) assays using a TCF4 antibody to analyze chromatin isolated from SKOV3.ip1, parental A2780 (lacking endogenous *WNT7A*), and A2780 cells overexpressing *WNT7A* (Figure 3d). DNA from the anti-TCF4 ChIP of SKOV3.ip1 was approximately 8-fold enriched in site 8, which contains the consensus TCF4 binding site located in the *1C* locus, when compared to IgG control. Interestingly, site 8 enrichment (5.5-fold) was observed in *WNT7A* overexpressing A2780 cells, but not in control A2780 cells. TCF/LEF binding sites in the promoters of *AXIN2* and *SP5*, well-known direct  $\beta$ -catenin/TCF target genes, were used as positive controls. Irrelevant sites ~4 kb and ~500 kb downstream of the *FGF1* locus (Non1 and Non2) and the *RPL19* locus on a different chromosome served as negative controls. Dominant negative (DN)-TCF4 expression in SKOV3.ip1 cells decreased *FGF1*, but not *WNT7A* levels (Supplementary Figure 4a). Specifically, *FGF1-1C* transcript expression was decreased in DN-TCF4 expressing cells (Supplementary Figure 4b), confirming the ChIP results in Figure 3d. Collectively, these results suggest that at least one site within the *FGF1* promoter is directly regulated by *WNT7A*/ $\beta$ -catenin/TCF in OvCa.

## WNT7A-FGF1 signaling promotes neoplastic transformation in OvCa

To understand whether FGF1 is necessary and/or sufficient for the effects of WNT7A in OvCa tumor progression, we generated stable WNT7A or FGF1 overexpressing or knockdown human OvCa cell lines (Supplementary Figure 5). Relative *WNT7A* and *FGF1* expression in a panel of OvCa cell lines was determined (Supplementary Figure 3) and A2780 cells were chosen for further analysis, as these cells have been widely used for gene manipulation and xenograft study, and showed lack of or low endogenous *WNT7A* and *FGF1*. The expression of FGF1 correlated with the upregulation of WNT7A in a genetically manipulated A2780 line, whereas WNT7A expression was not induced by FGF1 overexpression. Therefore, stable FGF1 knockdown in WNT7A overexpressing cells and their control cells were also generated.

Using these stable cell lines, we examined the *in vitro* effects of WNT7A and/or FGF1 on cell proliferation and adhesion (Supplementary Figure 6), using these assays as indicators of the roles of WNT7A and/or FGF1 in tumor growth *in vivo*. Cell doubling time was significantly shorter and ability to adhere to plastic was significantly greater in WNT7A overexpressing cells as compared to vector control cells. FGF1 overexpressing cells also exhibited a significant increase in cell adhesion, but no obvious decrease in cell doubling time was seen. However, FGF1 knockdown in WNT7A overexpressing cells showed that the effect of WNT7A on cell doubling time and adhesion was attenuated in the absence of FGF1.

Next, we examined the effects of WNT7A and/or FGF1 on tumor growth *in vivo*. Nude mice were intraperitoneally inoculated with control, WNT7A overexpressing, or FGF1 overexpressing cells (n=6 each group, Figure 4a). After 5 weeks, a significant increase in tumor burden, but not tumor number, was observed in mice injected with WNT7A or FGF1 overexpressing cells ( $1776.1 \pm 555.3$  mg or  $1275.8 \pm 396.2$  mg, respectively compared to pcDNA5,  $151.8 \pm 55.2$  mg), suggesting that both WNT7A and FGF1 have potential roles in tumor growth. The increased tumor growth by WNT7A overexpression was abrogated by inhibiting FGF1 (n=6 each group, Figure 4b), confirming that FGF1 is downstream of WNT7A signaling in OvCa cells. FGF1 knockdown in WNT7A overexpressing cells resulted in reduced tumor burden ( $265.3 \pm 106.5$  mg) compared to mice injected with cells overexpressing WNT7A and control shRNA ( $1372.8 \pm 474.4$  mg). We confirmed that expression of *WNT7A* and *FGF1* was maintained in orthotopic tumors.

## Nicosamide can inhibit WNT7A/ $\beta$ -catenin signaling in OvCa

Several WNT inhibitors have been found to effectively block WNT signaling.<sup>26–29</sup> To determine whether WNT7A/ $\beta$ -catenin signaling could be a therapeutic target in the context of OvCa treatment, we searched the LOPAC library containing 1280 pharmacological active compounds (Sigma-Aldrich, St. Louis, MO, USA) to find compounds inhibiting WNT signaling. A total of 14 small molecules were selected to determine WNT7A/ $\beta$ -catenin inhibitory activity in OvCa cell lines (Supplementary Figure 7a). Half of the small molecules significantly inhibited the activity of the TCF/LEF luciferase reporter in A2780 cells stimulated by WNT7A. Nicosamide exhibited the most significant inhibitory effect on WNT7A/ $\beta$ -catenin signaling. Thus, we chose to focus on nicosamide for further study.

Next, we assessed the molecular targets of niclosamide within the WNT/ $\beta$ -catenin signaling pathway in OvCa cells (Supplementary Figure 7bcd). Our results indicated potential regulation of WNT7A production, as niclosamide dose-dependently inhibited WNT7A levels. TCF/LEF reporter activity in cells stimulated by exogenous (A2780) or endogenous (SKOV3.ip1) WNT7A was suppressed by niclosamide. We also confirmed that niclosamide inhibited TCF/LEF activity stimulated by a constitutively active  $\beta$ -catenin (S33Y).

### Niclosamide regulates OvCa cell functions and inhibits tumor growth and progression

To determine whether niclosamide has therapeutic potential in OvCa, control and WNT7A knockdown SKOV3.ip1 cells<sup>9</sup> were used to assess cell proliferation, apoptosis, and migration (Figure 5). Niclosamide dose-dependently decreased cell number in SKOV3.ip1 cells, whereas cells depleted of WNT7A were less sensitive to the anti-proliferative effects of niclosamide (IC<sub>50</sub>=1.2 or 9.8  $\mu$ M in SKOV3.ip1 or WNT7A knockdown cells, respectively, Figure 5a). Similarly, cleaved-caspase 3 was increased up to 2.7-fold by treatment with 10  $\mu$ M niclosamide in SKOV3.ip1 cells, while WNT7A knockdown cells were less sensitive to this effect (Figure 5b). This result was confirmed by immunoblot analysis, showing that niclosamide increased cleaved caspase-3 and PARP, and decreased total caspase-3 and PARP. Niclosamide inhibited invasive features in SKOV3.ip1 cells (Figure 5c). It is well known that the SKOV3.ip1 cells primarily contain CDH1 (E-cadherin) negative cells. Our results showed that niclosamide dose-dependently increased CDH1 and decreased its transcriptional repressor SLUG in SKOV3.ip1, while niclosamide did not affect CDH1 and SLUG in WNT7A knockdown cells. Consistent with these results, migration was inhibited in WNT7A knockdown cells, and was dose-dependently decreased by niclosamide in parental SKOV3.ip1 cells.

We next determined the effect of niclosamide on ovarian tumor growth and progression (Figure 6). Five weeks after injection with SKOV3.ip1 cells, mice that received vehicle treatment (n=6) developed disseminated abdominal disease mimicking OvCa in patients. Niclosamide treated mice (n=6) had significantly fewer implants on the mesentery and intraperitoneal region (13.8  $\pm$  2.0 vs 78.5  $\pm$  8.7 implants) and their total tumor weight was 172  $\pm$  30 mg vs 936  $\pm$  121 mg. Decreased tumor cell proliferation, as determined by Ki67 immunohistochemistry, was correlated with tumor growth and quantitatively significant. TUNEL analysis revealed a significant number of apoptotic cells in the tumors of mice treated with niclosamide.

While niclosamide reduced *FGF1* expression in SKOV3.ip1 cells, FGF1 itself did not influence the efficacy of niclosamide (Supplementary Figure 8). When FGF1 only was overexpressed in A2780 cells, no differences in cell viability or death were observed compared to control following niclosamide exposure, whereas cells overexpressing WNT7A were more sensitive to the effects of niclosamide. Moreover, WNT7A overexpressing cells with and without FGF1 knockdown were equally sensitive to the effects of niclosamide, suggesting that niclosamide targets WNT7A/ $\beta$ -catenin rather than FGF1 directly. However, because FGF1 is a downstream target of aberrant WNT7A/ $\beta$ -catenin signaling and abundant WNT7A and FGF1 are observed in ovarian cancer, indirect downregulation of FGF1 by niclosamide remains clinically relevant.

## DISCUSSION

FGF1 has been identified as an adverse prognostic factor in OvCa risk.<sup>12–14</sup> In the present study, we show that *FGF1* is a downstream target of WNT7A signaling via  $\beta$ -catenin activation. First, FGF1 is abundant in OvCa, correlates with high *WNT7A*, especially in serous carcinomas. High expression of both *WNT7A* and *FGF1* is associated with poor survival (Figures 1 and 2). Second, the *FGF1* gene is directly regulated by WNT7A/ $\beta$ -catenin signaling (Figure 3). Third, FGF1 is sufficient to drive the tumor promoting effects of WNT7A (Figure 4).

Our previous study demonstrated that WNT7A is the sole ligand activating  $\beta$ -catenin/TCF signaling in OvCa.<sup>9</sup> We found that the *FGF1-IC* transcript is specifically regulated in a WNT7A and  $\beta$ -catenin/TCF-dependent manner in OvCa. The ChIP analysis indicates that a single consensus TCF/LEF binding site at the *IC* promoter locus is critical for WNT7A-mediated TCF binding, while binding sites within the *IA* and *IB* loci are not occupied in the context of WNT7A. It has been reported that *IC* and *ID* transcripts are potential markers for cell proliferation, while *IA* and *IB* are specific for the maintenance and survival of cells.<sup>24</sup> Although *FGF1-IC* specific functions in OvCa pathogenesis have yet to be determined, *FGF1-IC* is directly transcribed from activation of  $\beta$ -catenin/TCF signaling stimulated by WNT7A.

FGF1 binds receptors of FGFR1, 2, 3 and 4 with high-affinity.<sup>11</sup> Two receptors, FGFR2IIIb and FGFR4 have been implicated in OvCa progression,<sup>30, 31</sup> and FGFR4 has been identified as a potential therapeutic target in OvCa.<sup>31</sup> Several studies have reported that other members of the FGF family are WNT/ $\beta$ -catenin target genes. *FGF9* and *FGF20* are indirect and/or direct transcriptional targets of  $\beta$ -catenin/TCF signaling in endometrioid OvCa, in which the WNT pathway is often constitutively activated, usually via missense mutation of *CTNBI*.<sup>21, 32</sup> However, no members of the FGF family or the FGF receptors, other than FGF1, have been correlated with WNT7A expression in OvCa and none were directly regulated by WNT7A in our model. These results suggest that FGF1 is an important mediator of the tumor promoting events of WNT7A-dependent pathogenesis.

The importance of inappropriate WNT signaling for the development and progression of many cancers, including OvCa, has been well documented.<sup>7–9</sup> Therefore, it is plausible to search for therapeutic drugs that target the WNT7A/ $\beta$ -catenin-FGF1 pathway. While several small molecules that target this pathway have been identified<sup>33</sup> and, for a few of them, a precise mechanism of inhibition has been determined,<sup>27, 33, 34</sup> niclosamide was selected as the most efficient inhibitor of WNT7A-dependent TCF/LEF reporter activity. Niclosamide has recently been identified to target stem-like OvCa-initiating cells by a drug screening method, and gene expression array indicated involvement of WNT hyperactivity.<sup>35</sup> In the present study, we found that niclosamide could directly target  $\beta$ -catenin-TCF/LEF transcriptional activity, specifically; the effects of niclosamide on cell functions are more robust in WNT7A overexpressing cells. Our results also revealed that niclosamide reduced tumor growth and progression. We show that WNT7A is highest in serous carcinomas, the most common OvCa subtype,<sup>9</sup> and recent studies suggest niclosamide is effective in OvCa stem cells.<sup>35</sup> While the importance of WNT7A in OvCa stem cells is not known, WNT7A is

one of the critical factors determining cell fate in female reproductive development.<sup>36, 37</sup> The regulation of *WNT7A* in OvCa may lead us to understand the etiology and/or function of stem cells in aggressive serous carcinomas.

Although our results demonstrated that niclosamide efficacy in OvCa depended on *WNT7A*, but not *FGF1* function, other signaling pathways could be additional targets. Niclosamide is reported to target not only *WNT* signaling but also *mTORC1*, *STAT3* and *NFκB* pathways in several cancers.<sup>38–42</sup> Furthermore, we showed that niclosamide increased E-cadherin and decreased *SLUG* proteins. E-cadherin establishes cell polarity, mediates inhibition of proliferation and inhibits tumor cell growth.<sup>43, 44</sup> E-cadherin is often downregulated during tumor progression, leading to increased tumor invasiveness and metastasis.<sup>45, 46</sup> Therefore, it is likely that niclosamide reduces invasive and aggressive features in OvCa. While the potential interaction between these cascades and *WNT* signaling is an intriguing area for future study, overall niclosamide has broad potential as an effective inhibitor to treat OvCa patients.

In the present study, we determined that *WNT7A*-*FGF1* signaling is capable of inducing tumor growth, indicating a critical role in the aggressive progression of OvCa. Furthermore, we found that niclosamide is an effective therapeutic inhibitor of *WNT7A*/β-catenin signaling. New drugs are desperately needed to treat OvCa, and niclosamide is FDA-approved with a favorable safety profile. If niclosamide continues to hold promise in further pre-clinical studies, repurposing may ultimately prove to have a tremendous impact on the lives of OvCa patients in the clinical setting.

## MATERIALS AND METHODS

### Reagents and plasmids

Short hairpin RNAs (shRNA), cDNAs encoding human *WNT7A* and *FGF1*, and pcDNA5/FRT/V5-His, pcDNA6/TR and pcDNA5/TO plasmids were purchased from Sigma-Aldrich, Thermo Scientific (Rockford, IL, USA) and Life Technologies (Life Technologies, Grand Island, NY, USA), respectively. Niclosamide, iCRT3, iCRT14, Pyrvinium, Bafilomycin, Quercetin, NSC668036 and LiCl were purchased from Sigma-Aldrich. XAV939 and IWR were purchased from Cayman Chemical (Ann Arbor, MI, USA). IWP and Box5 were purchased from Thermo Scientific. ICG001, CCT031374 and iCRT5 were obtained from R&D Systems (Minneapolis, MN USA).

### Tissue samples and cell lines

Tissue microarray paraffin-embedded and fresh-frozen ovarian specimens were obtained from The University of Chicago and Southern Illinois University. Clinical and histopathologic information was collected and verified for each sample by a gynecologic pathologist following International Federation of Gynecology and Obstetrics (FIGO) classifications for stages I–IV.

OVCAR3, OVCAR5, SKOV3, TOV-112D, TOV-21G, OV-90, MDAH 2774 and ES2 cells were purchased from American Type Culture Collection (ATCC, Manassas, VA, USA). A2780 and OVCAR4 cells were purchased from Sigma-Aldrich and NCI, respectively.



KURAMOCHI, OVKATE and OVSAHO were purchased from JCRB cell bank (Osaka, Japan). HEY, HEYA8, OVCAR8, IGROV-1, OVCA420, OVCA429, OVCA432, OVCA433 and SKOV3.ip1 cells were purchased from the cell bank of The University of Texas MD Anderson Cancer Center. All cells were authenticated by short tandem repeat (STR) analysis and passaged within 6 months of receipt. All cells were tested routinely for cell proliferation and BrdU incorporation as well as mycoplasma contamination, and showed similar growth rates and negative mycoplasma throughout all experiments. TOV-112D, TOV-21G, and OV-90 cells were grown in 1:1 MCDB 105:M199 with 15% FBS and penicillin/streptomycin, other cells were cultured in DMEM with 10% FBS, 200mM glutamine and penicillin/streptomycin. All cell lines were grown at 37 °C in a humidified 5% CO<sub>2</sub> incubator.

DN-TCF4 expressing SKOV3.ip1 cells were generated using the T-REx system with pcDNA6/TR and pcDNA5/TO vectors (Life Technologies). A2780 cells were transfected with empty vector (pcDNA5/FRT), or plasmids encoding WNT7A tagged with V5 or FGF1 using the Flp-In system (Life Technologies). Hygromycin resistant stable clones were used for further analysis based on WNT7A and FGF1 expression detected by qPCR and western blot. Furthermore, stable FGF1 knockdown in WNT7A overexpressing cells and their control cells were generated using shRNA gene knockdown methods as described previously.<sup>9</sup> Stable clones doubly resistant for hygromycin and puromycin were selected and WNT7A and FGF1 expression were confirmed by qPCR and western blot.

#### **QPCR, western blot, TUNEL and cleaved-caspase assays**

Total RNA was isolated from tissues and cells, and cDNA was synthesized from total RNA. Relative gene expression was determined by SYBR green incorporation using a Bio-Rad myCycler as described previously.<sup>47</sup> A table of oligonucleotides used for each gene is presented in Supplementary Table 1. Ten micrograms of total protein from whole cell lysates were separated on SDS-PAGE gels and transferred to nitrocellulose membranes (EMD Millipore, Billerica, MA, USA). Membranes were blocked and incubated overnight at 4°C with primary antibodies. Bound antibody was visualized with IRDye 700 or 800 conjugated affinity-purified secondary antibodies (Rockland Immunochemicals, Gilbertsville, PA, USA) using the Odyssey infrared imaging system (LI-COR, Lincoln, NE, USA). A list of antibodies is shown in Supplementary Table 2. The TUNEL assay was performed according to manufacturer's instructions using ApopTag Fluorescein In Situ Apoptosis Detection Kit (Thermo Scientific). To assess apoptosis, cleaved-caspase 3 was quantitated using a PathScan Cleaved Caspase 3 Sandwich ELISA Kit according to manufacturer's instructions (Cell Signaling).

#### **Immunohistochemistry**

Immunolocalization of FGF1 in a total of 537 human specimens including 10 normal/benign (8 ovaries and 2 fallopian tubes), 147 serous, 20 endometrioid, 22 clear cell, 7 mucinous and 32 fallopian tube primary tumors, and 299 metastases from 199 serous, 8 endometrioid, 15 clear cell, 4 mucinous and 73 fallopian tube tumors; and Ki67 in xenografts from nude mice were examined in cross-sections (5 µm) of paraffin-embedded tissue sections using specific primary antibodies and a Vectastain Elite ABC Kit (Vector laboratories, Burlingame, CA,

USA). Immunostaining was semiquantitatively scored by Image J, which is a public domain Java image processing program developed by NIH.

### Cell proliferation, adhesion and migration

Cell proliferation, adhesion and migration assays were performed following our previously described methods.<sup>9, 48</sup> To assess cell proliferation, cells ( $2 \times 10^4$ /well) were seeded in 24-well plates. Doubling time of cells was calculated from the growth rate during the exponential growth phase (0–72 h) using the formula,  $Td = 0.693t/\ln(N_t/N_0)$ , where  $t$  is time in days,  $N_t$  is cell number at time  $t$ , and  $N_0$  is cell number at the initial time.<sup>49, 50</sup> To determine the effect of niclosamide on cell viability, cells were treated with vehicle (0.1% DMSO) or niclosamide (0–10  $\mu$ M) for 48 hours before being harvested and counted by trypan blue exclusion. To assess cell adhesion, cells ( $1 \times 10^5$ /well) were seeded in 24-well plates and harvested after 1 h incubation. Cell migration assays were performed using a modified Boyden Chamber method with 8- $\mu$ m pore size polycarbonate membrane 24-well transwells. Cells were treated with vehicle or niclosamide for 24 hours before being harvested, re-plated ( $75 \times 10^3$  cells per well in 100  $\mu$ l of serum-free medium) into upper wells, and placed in lower wells containing 500  $\mu$ l serum-free medium in order to determine unstimulated migratory ability.

### Chromatin immunoprecipitation assay

ChIP assays were performed using the Magna ChIP G-chromatin immunoprecipitation Kit (Thermo Scientific) as described previously.<sup>51</sup> Sheared chromatin from  $1 \times 10^6$  cells was immunoprecipitated with mouse monoclonal TCF4 antibody or control mouse IgG (Thermo Scientific). Primers for the qPCR are listed in Supplementary Table 3.

### Animal experiments

For *in vivo* animal studies, 7–8 week-old female nude mice (*nu/nu* BALB/c, Jackson Laboratories) were injected with  $1 \times 10^6$  cells i.p. in a total volume of 400  $\mu$ l. Body weights were monitored every 7 days thereafter. Mice were euthanized and necropsied 5 weeks after injection. Niclosamide (200 mg/kg B.W.) or vehicle control (PEG400) was given daily by oral gavage for 5 weeks. Harvested tumors were either frozen or fixed with 4% paraformaldehyde in PBS for further analysis.

### Statistical analyses

Quantitative data were subjected to least-squares ANOVA and differences between individual means were tested by a Tukey multiple-range test using Prism 4.0 (Graphpad, San Diego, CA, USA). QPCR data were corrected for differences in sample loading using the *RPL19* data as a covariate. Tests of significance were performed using the appropriate error terms according to the expectation of the mean squares for error. A p-value of 0.05 or less was considered significant. Data are presented as least-square means (LSM) with standard error of the means (SEM). The Kaplan-Meier method was used to calculate the survival rates and was evaluated by the log-rank test using GEO and TCGA datasets: GSE9891,<sup>52</sup> GSE14764,<sup>53</sup> GSE26712<sup>54</sup> and TCGA-OV, that contained 285, 80, 195 and 570 samples of normal and cancerous ovary, peripheral tissues and fallopian tubes, respectively. A total of

961 primary ovarian tumors with completed data sets (151, 68, 185 and 557 from GSE9891, GSE14764, GSE26712 and TCGA-OV, respectively) were selected for survival analysis.

## Supplementary Material

Refer to Web version on PubMed Central for supplementary material.

## Acknowledgments

We thank Gail Isenberg for editing the manuscript. This work was supported by NIH/NCI CA179214 and ACS-IL 139038 (to KH), and NIH/NICHHD HD065584 (to JAM).

## References

1. Siegel R, Ma J, Zou Z, Jemal A. Cancer statistics, 2014. *CA: a cancer journal for clinicians*. 2014; 64:9–29. [PubMed: 24399786]
2. Goff BA, Mandel LS, Melancon CH, Muntz HG. Frequency of symptoms of ovarian cancer in women presenting to primary care clinics. *Jama*. 2004; 291:2705–2712. [PubMed: 15187051]
3. Teo R, Mohrlen F, Plickert G, Muller WA, Frank U. An evolutionary conserved role of Wnt signaling in stem cell fate decision. *Developmental biology*. 2006; 289:91–99. [PubMed: 16309665]
4. Polakis P. Wnt signaling and cancer. *Genes & development*. 2000; 14:1837–1851. [PubMed: 10921899]
5. Liu W, Xing F, Iizumi-Gairani M, Okuda H, Watabe M, Pai SK, et al. N-myc downstream regulated gene 1 modulates Wnt-beta-catenin signalling and pleiotropically suppresses metastasis. *EMBO molecular medicine*. 2012; 4:93–108. [PubMed: 22246988]
6. Polakis P. The many ways of Wnt in cancer. *Current opinion in genetics & development*. 2007; 17:45–51. [PubMed: 17208432]
7. Gateliffe TA, Monk BJ, Planutis K, Holcombe RF. Wnt signaling in ovarian tumorigenesis. *Int J Gynecol Cancer*. 2008; 18:954–962. [PubMed: 17986238]
8. Arend RC, Londono-Joshi AI, Straughn JM Jr, Buchsbaum DJ. The Wnt/beta-catenin pathway in ovarian cancer: a review. *Gynecologic oncology*. 2013; 131:772–779. [PubMed: 24125749]
9. Yoshioka S, King ML, Ran S, Okuda H, MacLean JA 2nd, McAsey ME, et al. WNT7A regulates tumor growth and progression in ovarian cancer through the WNT/beta-catenin pathway. *Mol Cancer Res*. 2012; 10:469–482. [PubMed: 22232518]
10. Friesel RE, Maciag T. Molecular mechanisms of angiogenesis: fibroblast growth factor signal transduction. *Faseb J*. 1995; 9:919–925. [PubMed: 7542215]
11. Powers CJ, McLeskey SW, Wellstein A. Fibroblast growth factors, their receptors and signaling. *Endocrine-related cancer*. 2000; 7:165–197. [PubMed: 11021964]
12. Birrer MJ, Johnson ME, Hao K, Wong KK, Park DC, Bell A, et al. Whole genome oligonucleotide-based array comparative genomic hybridization analysis identified fibroblast growth factor 1 as a prognostic marker for advanced-stage serous ovarian adenocarcinomas. *J Clin Oncol*. 2007; 25:2281–2287. [PubMed: 17538174]
13. Meng QH, Xu E, Hildebrandt MA, Liang D, Lu K, Ye Y, et al. Genetic variants in the fibroblast growth factor pathway as potential markers of ovarian cancer risk, therapeutic response, and clinical outcome. *Clinical chemistry*. 2014; 60:222–232. [PubMed: 24146310]
14. Smith G, Ng MT, Shepherd L, Herrington CS, Gourley C, Ferguson MJ, et al. Individuality in FGF1 expression significantly influences platinum resistance and progression-free survival in ovarian cancer. *British journal of cancer*. 2012
15. Lu W, Lin C, Roberts MJ, Waud WR, Piazza GA, Li Y. Niclosamide suppresses cancer cell growth by inducing Wnt co-receptor LRP6 degradation and inhibiting the Wnt/beta-catenin pathway. *PLoS one*. 2011; 6:e29290. [PubMed: 22195040]

16. Mook RA Jr, Chen M, Lu J, Barak LS, Lyerly HK, Chen W. Small molecule modulators of Wnt/ beta-catenin signaling. *Bioorganic & medicinal chemistry letters*. 2013; 23:2187–2191. [PubMed: 23453073]
17. Osada T, Chen M, Yang XY, Spasojevic I, Vandeuken JB, Hsu D, et al. Antihelminth compound niclosamide downregulates Wnt signaling and elicits antitumor responses in tumors with activating APC mutations. *Cancer research*. 2011; 71:4172–4182. [PubMed: 21531761]
18. Sack U, Walther W, Scudiero D, Selby M, Kobelt D, Lemm M, et al. Novel effect of antihelminthic Niclosamide on S100A4-mediated metastatic progression in colon cancer. *Journal of the National Cancer Institute*. 2011; 103:1018–1036. [PubMed: 21685359]
19. Wieland A, Trageser D, Gogolok S, Reinartz R, Hofer H, Keller M, et al. Anticancer effects of niclosamide in human glioblastoma. *Clin Cancer Res*. 2013; 19:4124–4136. [PubMed: 23908450]
20. Chen M, Wang J, Lu J, Bond MC, Ren XR, Lyerly HK, et al. The anti-helminthic niclosamide inhibits Wnt/ Frizzled1 signaling. *Biochemistry*. 2009; 48:10267–10274. [PubMed: 19772353]
21. Hendrix ND, Wu R, Kuick R, Schwartz DR, Fearon ER, Cho KR. Fibroblast growth factor 9 has oncogenic activity and is a downstream target of Wnt signaling in ovarian endometrioid adenocarcinomas. *Cancer research*. 2006; 66:1354–1362. [PubMed: 16452189]
22. Aletti GD, Gallenberg MM, Cliby WA, Jatoi A, Hartmann LC. Current management strategies for ovarian cancer. *Mayo Clinic proceedings*. 2007; 82:751–770. [PubMed: 17550756]
23. Parkin DM, Bray F, Ferlay J, Pisani P. Global cancer statistics, 2002. *CA: a cancer journal for clinicians*. 2005; 55:74–108. [PubMed: 15761078]
24. Chotani MA, Chiu IM. Differential regulation of human fibroblast growth factor 1 transcripts provides a distinct mechanism of cell-specific growth factor expression. *Cell Growth Differ*. 1997; 8:999–1013. [PubMed: 9300182]
25. Madiari F, Hackshaw KV, Chiu IM. Characterization of the entire transcription unit of the mouse fibroblast growth factor 1 (FGF-1) gene. Tissue-specific expression of the FGF-1. *A mRNA The Journal of biological chemistry*. 1999; 274:11937–11944. [PubMed: 10207015]
26. Barker N, Clevers H. Mining the Wnt pathway for cancer therapeutics. *Nature reviews*. 2006; 5:997–1014.
27. Chen W, Chen M, Barak LS. Development of small molecules targeting the Wnt pathway for the treatment of colon cancer: a high-throughput screening approach. *American journal of physiology Gastrointestinal and liver physiology*. 2010; 299:G293–300. [PubMed: 20508156]
28. Dodge ME, Lum L. Drugging the cancer stem cell compartment: lessons learned from the hedgehog and Wnt signal transduction pathways. *Annual review of pharmacology and toxicology*. 2011; 51:289–310.
29. Meijer L, Flajolet M, Greengard P. Pharmacological inhibitors of glycogen synthase kinase 3. *Trends in pharmacological sciences*. 2004; 25:471–480. [PubMed: 15559249]
30. Steele IA, Edmondson RJ, Bulmer JN, Bolger BS, Leung HY, Davies BR. Induction of FGF receptor 2-IIIb expression and response to its ligands in epithelial ovarian cancer. *Oncogene*. 2001; 20:5878–5887. [PubMed: 11593393]
31. Zaid TM, Yeung TL, Thompson MS, Leung CS, Harding T, Co NN, et al. Identification of FGFR4 as a potential therapeutic target for advanced-stage, high-grade serous ovarian cancer. *Clin Cancer Res*. 2013; 19:809–820. [PubMed: 23344261]
32. Chamorro MN, Schwartz DR, Vonica A, Brivanlou AH, Cho KR, Varmus HE. FGF-20 and DKK1 are transcriptional targets of beta-catenin and FGF-20 is implicated in cancer and development. *The EMBO journal*. 2005; 24:73–84. [PubMed: 15592430]
33. Curtin JC, Lorenzi MV. Drug discovery approaches to target Wnt signaling in cancer stem cells. *Oncotarget*. 2010; 1:563–577.
34. Huang SM, Mishina YM, Liu S, Cheung A, Stegmeier F, Michaud GA, et al. Tankyrase inhibition stabilizes axin and antagonizes Wnt signalling. *Nature*. 2009; 461:614–620. [PubMed: 19759537]
35. Yo YT, Lin YW, Wang YC, Balch C, Huang RL, Chan MW, et al. Growth inhibition of ovarian tumor-initiating cells by niclosamide. *Molecular cancer therapeutics*. 2012; 11:1703–1712. [PubMed: 22576131]

36. Cooke PS, Spencer TE, Bartol FF, Hayashi K. Uterine glands: development, function and experimental model systems. *Molecular human reproduction*. 2013; 19:547–558. [PubMed: 23619340]
37. Sassoon D. Wnt genes and endocrine disruption of the female reproductive tract: a genetic approach. *Mol Cell Endocrinol*. 1999; 158:1–5. [PubMed: 10630399]
38. Balgi AD, Fonseca BD, Donohue E, Tsang TC, Lajoie P, Proud CG, et al. Screen for chemical modulators of autophagy reveals novel therapeutic inhibitors of mTORC1 signaling. *PLoS one*. 2009; 4:e7124. [PubMed: 19771169]
39. Fonseca BD, Diering GH, Bidinosti MA, Dalal K, Alain T, Balgi AD, et al. Structure-activity analysis of niclosamide reveals potential role for cytoplasmic pH in control of mammalian target of rapamycin complex 1 (mTORC1) signaling. *The Journal of biological chemistry*. 2012; 287:17530–17545. [PubMed: 22474287]
40. Jin Y, Lu Z, Ding K, Li J, Du X, Chen C, et al. Antineoplastic mechanisms of niclosamide in acute myelogenous leukemia stem cells: inactivation of the NF-kappaB pathway and generation of reactive oxygen species. *Cancer research*. 2010; 70:2516–2527. [PubMed: 20215516]
41. Li R, Hu Z, Sun SY, Chen ZG, Owonikoko TK, Sica GL, et al. Niclosamide overcomes acquired resistance to erlotinib through suppression of STAT3 in non-small cell lung cancer. *Molecular cancer therapeutics*. 2013; 12:2200–2212. [PubMed: 23894143]
42. You S, Li R, Park D, Xie M, Sica GL, Cao Y, et al. Disruption of STAT3 by niclosamide reverses radioresistance of human lung cancer. *Molecular cancer therapeutics*. 2014; 13:606–616. [PubMed: 24362463]
43. Kim NG, Koh E, Chen X, Gumbiner BM. E-cadherin mediates contact inhibition of proliferation through Hippo signaling-pathway components. *Proceedings of the National Academy of Sciences of the United States of America*. 2011; 108:11930–11935. [PubMed: 21730131]
44. Lau MT, Klausen C, Leung PC. E-cadherin inhibits tumor cell growth by suppressing PI3K/Akt signaling via beta-catenin-Egr1-mediated PTEN expression. *Oncogene*. 2011; 30:2753–2766. [PubMed: 21297666]
45. Perl AK, Wilgenbus P, Dahl U, Semb H, Christofori G. A causal role for E-cadherin in the transition from adenoma to carcinoma. *Nature*. 1998; 392:190–193. [PubMed: 9515965]
46. Takeichi M. Cadherins in cancer: implications for invasion and metastasis. *Current opinion in cell biology*. 1993; 5:806–811. [PubMed: 8240824]
47. Hayashi K, Erikson DW, Tilford SA, Bany BM, Maclean JA 2nd, Rucker EB 3rd, et al. Wnt genes in the mouse uterus: potential regulation of implantation. *Biology of reproduction*. 2009; 80:989–1000. [PubMed: 19164167]
48. Hayashi K, Burghardt RC, Bazer FW, Spencer TE. WNTs in the ovine uterus: potential regulation of periimplantation ovine conceptus development. *Endocrinology*. 2007; 148:3496–3506. [PubMed: 17431004]
49. Chauhan SC, Vannatta K, Ebeling MC, Vinayek N, Watanabe A, Pandey KK, et al. Expression and functions of transmembrane mucin MUC13 in ovarian cancer. *Cancer research*. 2009; 69:765–774. [PubMed: 19176398]
50. Singh AP, Moniaux N, Chauhan SC, Meza JL, Batra SK. Inhibition of MUC4 expression suppresses pancreatic tumor cell growth and metastasis. *Cancer research*. 2004; 64:622–630. [PubMed: 14744777]
51. Maclean JA 2nd, Hu Z, Welborn JP, Song HW, Rao MK, Wayne CM, et al. The RHOX Homeodomain Proteins Regulate the Expression of Insulin and Other Metabolic Regulators in the Testis. *The Journal of biological chemistry*. 2013
52. Tothill RW, Tinker AV, George J, Brown R, Fox SB, Lade S, et al. Novel molecular subtypes of serous and endometrioid ovarian cancer linked to clinical outcome. *Clin Cancer Res*. 2008; 14:5198–5208. [PubMed: 18698038]
53. Denkert C, Budczies J, Darb-Esfahani S, Gyorffy B, Sehouli J, Konsgen D, et al. A prognostic gene expression index in ovarian cancer - validation across different independent data sets. *The Journal of pathology*. 2009; 218:273–280. [PubMed: 19294737]

54. Bonome T, Levine DA, Shih J, Randonovich M, Pise-Masison CA, Bogomolny F, et al. A gene signature predicting for survival in suboptimally debulked patients with ovarian cancer. *Cancer research*. 2008; 68:5478–5486. [PubMed: 18593951]

Author Manuscript

Author Manuscript

Author Manuscript

Author Manuscript

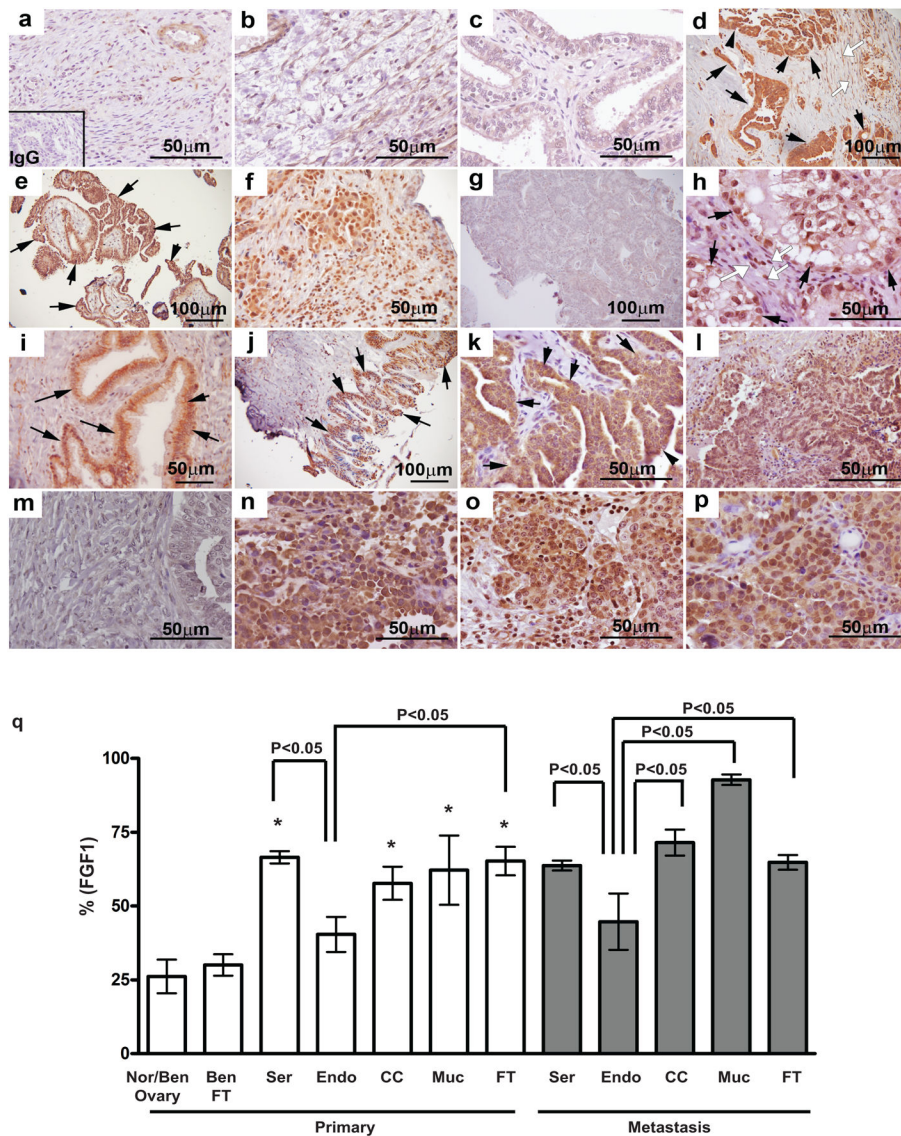


**Figure 1.**

Analysis of FGF1 in ovarian cancer. (a–p) Representative photomicrographs of immunoreactive FGF1 in normal/benign, primary and metastasized ovarian and fallopian tube tumors (A total of 537 specimens including 10 normal/benign (8 ovaries and 2 fallopian tubes), 147 serous, 20 endometrioid, 22 clear cell, 7 mucinous and 32 fallopian tube primary tumors, and 299 metastasized tumors from 199 serous, 8 endometrioid, 15 clear cell, 4 mucinous and 73 fallopian tubes). (a) Normal ovary. (b) Benign ovary. (c) Benign fallopian tube. (d) Black arrows point to high grade invasive serous epithelial cells. Open white arrows point to fibroblasts. (e) Black arrows point to epithelial cells of low grade serous carcinoma. (f) Serous carcinoma lymphocytes. (g) Endometrioid carcinoma. (h) Black arrows point to epithelial cells of clear cell carcinoma. Open white arrows point to fibroblasts. (i) Black arrows point to non-invasive cells lining the basal membrane of mucinous carcinoma. (j) Black arrows point to surface epithelium of mucinous carcinoma. (k) Black arrows point to epithelial fallopian tube carcinoma. (l) Serous carcinoma

metastasis in peritoneum. (m) Endometrioid carcinoma metastasis in omentum. (n) Clear cell carcinoma metastasis in peritoneum. (o) Mucinous carcinoma metastasis in omentum. (p) Fallopian tube carcinoma metastasis in ovary. (q) Immunoreactive FGF1 levels were quantitatively scored by Image J analysis. Nor/Ben, normal/benign; Ser, serous; Endo, endometrioid; CC, clear cell; Muc, mucinous; FT, fallopian tube. \*P<0.05 vs. normal/benign ovaries and fallopian tubes.

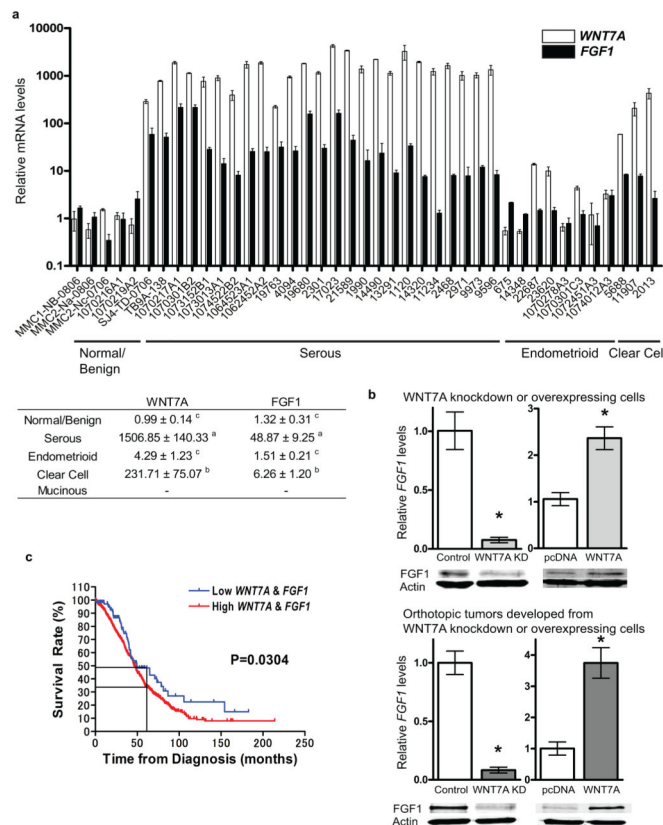
Author Manuscript

Author Manuscript

Author Manuscript

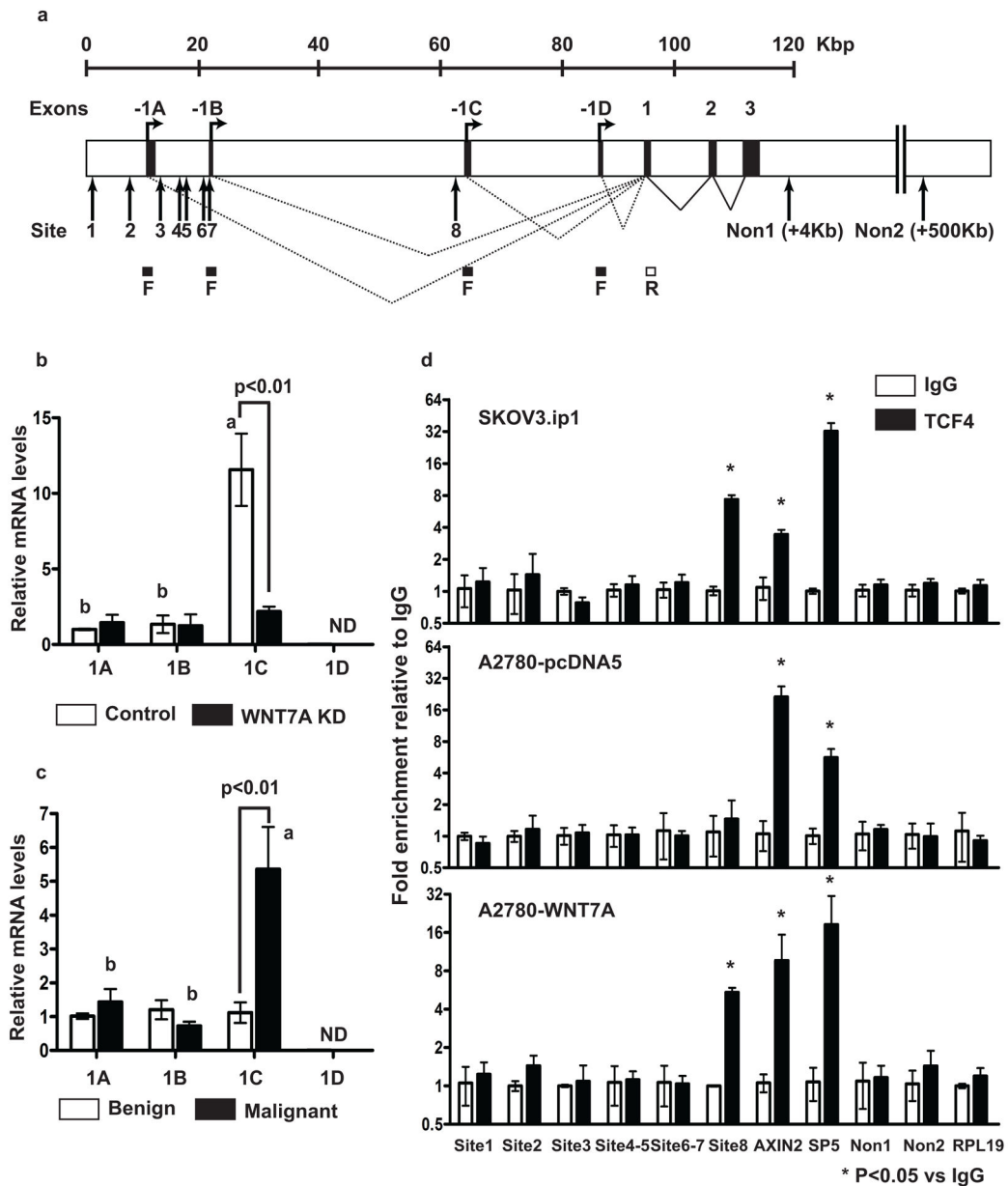
Author Manuscript





**Figure 2.**

Expression of FGF1 correlates with WNT7A in ovarian cancer. (a) Relative *WNT7A* and *FGF1* expression. A total of 41 fresh-frozen ovarian samples including 5 normal/benign, 25 serous, 8 endometrioid, 3 clear cell and 0 mucinous were examined for *WNT7A* and *FGF1* levels. Duplicates of each sample were analyzed by qPCR. Values were normalized against *RPL19* and are expressed as fold above normal/benign ( $\pm$  SEM), which was arbitrarily given a value of 1. Mean values from each subtype are shown in table. Different letters denote transcripts that have statistically significant ( $P < 0.01$ ) differences in mean expression levels. (b) Relative FGF1 mRNA and protein expression in WNT7A knockdown SKOV3.ip1 cells and WNT7A overexpressing SKOV3 cells. \* $P < 0.05$  vs. control or pcDNA. Relative FGF1 mRNA and protein expression in orthotopic tumors developed from WNT7A knockdown SKOV3.ip1 cells or WNT7A overexpressing SKOV3 cells. \* $P < 0.05$  vs. control or pcDNA. (c) WNT7A and FGF1 expression correlates with survival. Overall survival rate was calculated in 151, 68, 185, 557 patients from GSE9891, GSE14764, GSE26712 and TCGA-OV, respectively, in relation to the expression of *WNT7A* and *FGF1* by Kaplan-Meier method using Prism 4.0. The P-value was determined by the log rank test.

**Figure 3.**

FGF1 is a direct  $\beta$ -catenin/TCF target. (a) Human *FGF1* gene and transcripts. Alternative splicing of untranslated exons (*1A*, *1B*, *1C* and *1D*) to exon 1 will generate mRNAs *1A*, *1B*, *1C* and *1D*. A total of 8 consensus TCF/LEF-binding elements (WWCAAWG, W=A/T) at the *FGF1* genomic locus are shown. F; forward primers designed in *1A*, *1B*, *1C* or *1D* and R; reverse primer designed in exon 1. Relative *FGF1* alternative splicing mRNA levels in (b) control and WNT7A knockdown SKOV3.ip1 cells, and (c) human ovarian normal/benign (n=5) and malignant (n=36) tumors. Different letters denote transcripts that have statistically significant ( $P < 0.01$ ) differences in mean expression levels. ND: non detectable. (d) ChIP assay of DNA isolated from SKOV3.ip1, A2780-pcDNA5 and WNT7A overexpressing cells immunoprecipitated with TCF4 antibody. Immunoprecipitated DNA

was analyzed by qPCR and normalized to input. TCF4 binding sites at AXIN2 and SP5 loci were used as positive controls. Three irrelevant non TCF4 binding sites on the same chromosome of *FGF1* and different chromosome at the *RPL19* locus were used as negative controls.

Author Manuscript

Author Manuscript

Author Manuscript

Author Manuscript

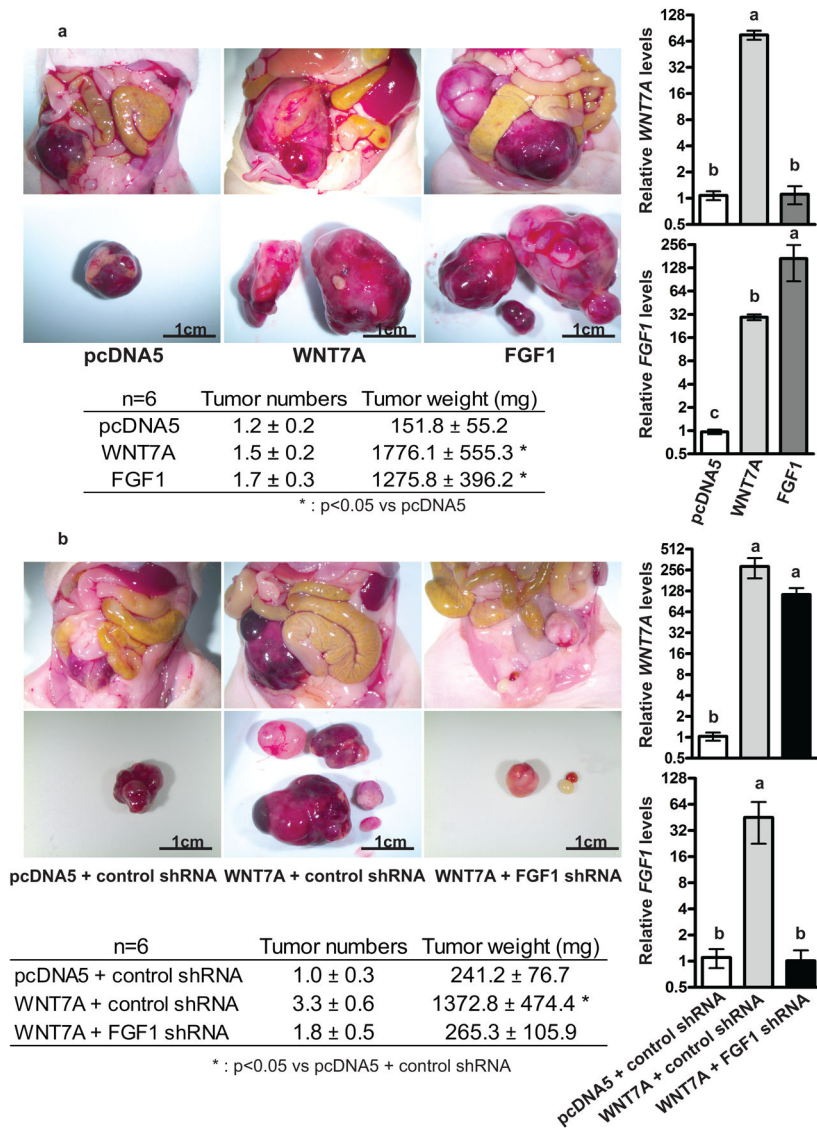


**Figure 4.**

FGF1 promotes the tumorigenic functions of WNT7A. (a) WNT7A or FGF1 overexpression increased tumor growth. Nude mice were injected i.p. with vector control cells, WNT7A overexpressing, or FGF1 overexpressing cells. The images provide a direct view of the abdominopelvic cavity and tumors isolated from mice. Total tumor numbers and weight 5 weeks after i.p. injection are shown (n=6 each group). Relative *WNT7A* or *FGF1* expression in orthotopic tumors that developed from vector control, WNT7A overexpressing, or FGF1 overexpressing cells. Different letters denote groups that have statistically significant (P<0.05) differences in mean expression levels. (b) FGF1 knockdown inhibits WNT7A-dependent tumor growth. FGF1 knockdown in WNT7A overexpressing cells inhibited tumor growth. Nude mice were injected i.p. with vector control, or control or FGF1 knockdown WNT7A overexpressing cells. The images provide a direct view of the abdominopelvic cavity and tumors isolated from the mice. Total tumor numbers and weight 5 weeks after i.p. injection are shown (n=6 each group). Relative *WNT7A* or *FGF1* expression in orthotopic

tumors that developed from vector control, or control or FGF1 knockdown WNT7A overexpressing cells. Different letters denote groups that have statistically significant ( $P < 0.05$ ) differences in mean expression levels.

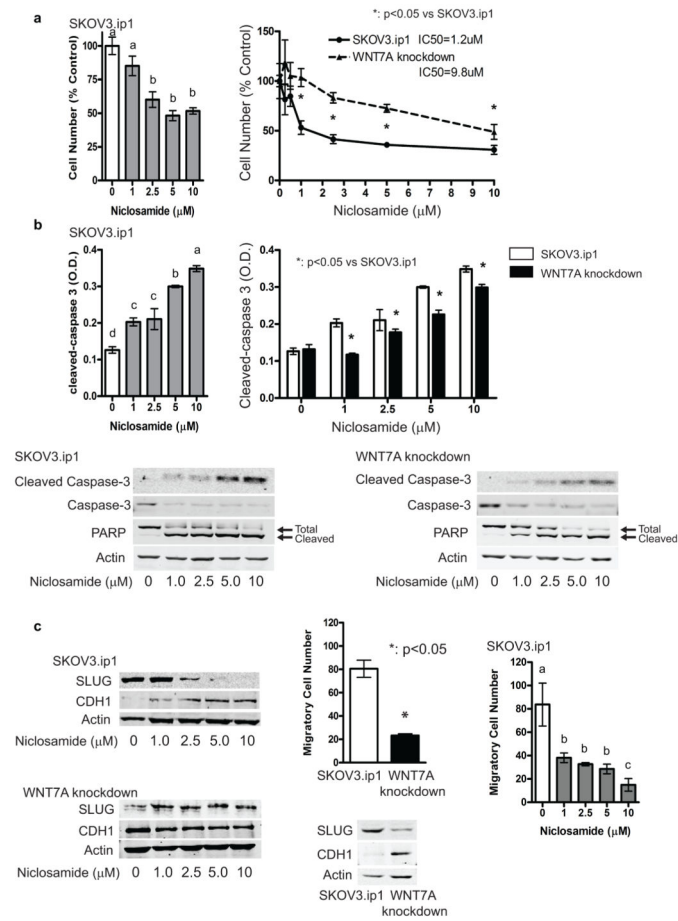
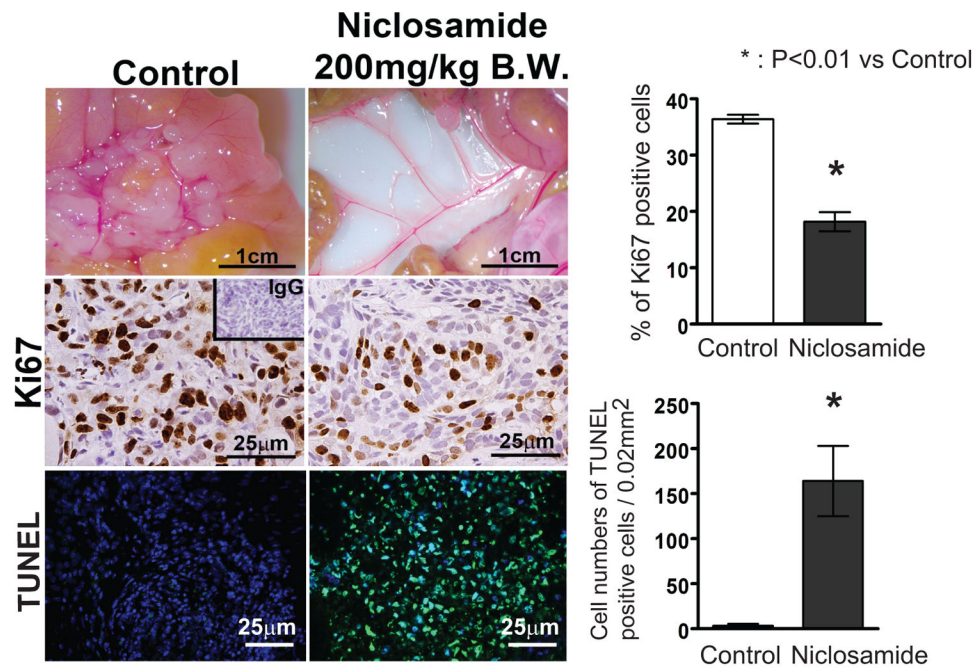


**Figure 5.**

Niclosamide effectively inhibits ovarian cancer cell functions in WNT7A expressing cells. (a) Effects of niclosamide on cell viability in SKOV3.ip1 control and WNT7A knockdown cells. Different letters denote groups that have statistically significant ( $P < 0.05$ ) differences in mean cell number. (b) Effects of niclosamide on cleavage of the apoptosis effector molecule caspase-3 and its target PARP in SKOV3.ip1 and WNT7A knockdown cells by ELISA and/or western blots. Different letters denote groups that have statistically significant ( $P < 0.05$ ) differences in mean O.D. (c) Effects of niclosamide on CDH1 and SLUG expression levels, and cell migration in SKOV3.ip1 control and WNT7A knockdown cells. Different letters denote groups that have statistically significant ( $P < 0.05$ ) differences in mean cell number.



n=6	Tumor numbers	Tumor weight (mg)
Control	78.5 ± 8.7	936 ± 121
Niclosamide (200mg/kg B.W.)	13.8 ± 2.0 *	172 ± 30 *

\* : p<0.01 vs control

**Figure 6.**

Effects of niclosamide on tumor growth in ovarian cancer. (a) Mice were injected i.p. with SKOV3.ip1 cells and treated with niclosamide (0 and 200 mg/kg/day B.W.) by oral gavage for 5 weeks starting 3 days after i.p. injection. Tumor implant number and total tumor weight 5 weeks after niclosamide treatment are shown (n=6 each group). Cell proliferation and apoptosis were determined by immunoreactive Ki67 staining and TUNEL assay.